

Structural Acoustic Physics-Based Modeling of Curved Composite Shells

Rachel E. Hesse
Ranges, Engineering, and Analysis Department



**Naval Undersea Warfare Center Division
Newport, Rhode Island**

Approved for public release; distribution is unlimited.

PREFACE

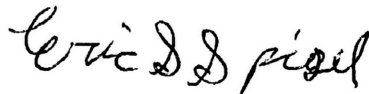
This document was prepared under NUWC Division Newport Internal Investment Program, NWA 300000111145/0010. The principal investigator is Rachel E. Hesse (Code 7023).

The technical reviewer for this report was Matthew E. Johnson (Code 7023).

ACKNOWLEDGMENTS

The author gratefully acknowledges Paul V. Cavallaro (Code 7023), Andrew W. Hulton (Code 7023), Daniel Perez (1533), and Matthew E. Johnson (Code 7023) for their support in developing this research, as well as the Office of Naval Research and Neil. J. Dubois (Code 00T1) for funding this research.

Reviewed and Approved: 13 September 2017



Eric S. Spigel
Head, Ranges, Engineering, and Analysis Department



REPORT DOCUMENTATION PAGE					Form Approved OMB No. 0704-0188	
<p>The public reporting burden for this collection of information is estimated to average 1 hour per response, including the time for reviewing instructions, searching existing data sources, gathering and maintaining the data needed, and completing and reviewing the collection of information. Send comments regarding this burden estimate or any other aspect of this collection of information, including suggestions for reducing this burden, to Department of Defense, Washington Headquarters Services, Directorate for Information Operations and Reports (0704-0188), 1215 Jefferson Davis Highway, Suite 1204, Arlington, VA 22202-4302. Respondents should be aware that notwithstanding any other provision of law, no person shall be subject to any penalty for failing to comply with a collection of information if it does not display a currently valid OPM control number.</p> <p>PLEASE DO NOT RETURN YOUR FORM TO THE ABOVE ADDRESS.</p>						
1. REPORT DATE (DD-MM-YYYY) 19-09-2017		2. REPORT TYPE Technical Report		3. DATES COVERED (From – To)		
4. TITLE AND SUBTITLE Structural Acoustic Physics-Based Modeling of Curved Composite Shells				5a. CONTRACT NUMBER		
				5b. GRANT NUMBER		
				5c. PROGRAM ELEMENT NUMBER		
6. AUTHOR(S) Rachel E. Hesse				5d. PROJECT NUMBER		
				5e. TASK NUMBER		
				5f. WORK UNIT NUMBER		
7. PERFORMING ORGANIZATION NAME(S) AND ADDRESS(ES) Naval Undersea Warfare Center Division Newport 1176 Howell Street Newport, RI 02841-1708				8. PERFORMING ORGANIZATION REPORT NUMBER TR 12,236		
9. SPONSORING/MONITORING AGENCY NAME(S) AND ADDRESS(ES) Naval Undersea Warfare Center Division Newport 1176 Howell Street Newport, RI 02841-1708				10. SPONSORING/MONITOR'S ACRONYM NUWC		
				11. SPONSORING/MONITORING REPORT NUMBER		
12. DISTRIBUTION/AVAILABILITY STATEMENT Approved for public release; distribution is unlimited.						
13. SUPPLEMENTARY NOTES						
14. ABSTRACT <p>Understanding sound wave propagation through a curved shell geometry is essential for a wide variety of underwater applications. The objective of this study was to use physics-based modeling (PBM) to investigate wave propagations through curved shells that are subjected to acoustic excitation. An improved understanding of the absorption and reflection properties of materials, such as fiber-reinforced polymer (FRP) composites, will enhance the design methods for a variety of Navy products such as acoustic sensors, acoustic windows, and unmanned underwater vehicles.</p> <p>The research documented in this report investigates the reflection and transmission coefficients of both flat plates and curved shells for steel and composite materials. Results show that the finite element computational models accurately match analytical calculations, and that the composite material studied in this report has more desirable reflection and absorption properties than steel for typical Navy applications. This research also explores the use of coupled Eulerian-Lagrangian (CEL) and smoothed particle hydrodynamics (SPH) modeling approaches in place of the current, traditional Lagrangian approach. Unfortunately, these approaches were found to be unsuitable for the type of acoustic analyses performed throughout this research. However, results from the traditional Lagrangian approach confirmed the validity of current modeling techniques and allowed for the study of the acoustic properties of various geometries and materials. This can help drive future research on composite material applications and enhance design methods for future Navy products.</p>						
15. SUBJECT TERMS Finite Element Analysis, Structural Acoustics, Fiber-Reinforced Composites, Physics-Based Modeling						
16. SECURITY CLASSIFICATION OF:			17. LIMITATION OF ABSTRACT	18. NUMBER OF PAGES	19a. NAME OF RESPONSIBLE PERSON	
a. REPORT	b. ABSTRACT	c. THIS PAGE			Rachel E. Hesse	
(U)	(U)	(U)	SAR	27	19b. TELEPHONE NUMBER (Include area code) 401-832-4906	

TABLE OF CONTENTS

Section	Page
LIST OF TABLES	ii
LIST OF ABBREVIATIONS AND ACRONYMS	ii
LIST OF SYMBOLS	iii
1 INTRODUCTION	1
2 PROJECT APPROACH	2
3 ANALYTICAL CALCULATIONS	2
4 FINITE ELEMENT MODEL DESCRIPTION	5
4.1 Flat Plate Model	5
4.2 Curved Shell Model	7
5 RESULTS	9
5.1 Comparison of Flat Plate Computational Models to Analytical Calculations	9
5.2 Curved Shell Results	11
6 CEL/SPH ANALYSIS TECHNIQUES	16
6.1 Coupled Eulerian-Lagrangian Analysis	16
6.2 Smoothed Particle Hydrodynamics Analysis	17
7 CONCLUSION	19
REFERENCES	21

LIST OF ILLUSTRATIONS

Figure	Page
1 Depiction of Fluid Layer Orientation and Acoustic Wave Transmission	3
2 Flat Plate 3D Finite Element Model with a 1-Inch Plate	5
3 Closeup View of Mesh Refinement for a Flat Plate Model	6
4 Curved Shell 2D Plane Strain Model with 1-Inch Shell	8
5 Closeup of a Mesh Refinement in a 1-Inch Curved Shell Model	9
6 R and T Coefficients versus Frequency for a 1-Inch Flat Plate	10
7 R and T Coefficients versus Frequency for a 2-Inch Flat Plate	11
8 Depiction of Normal Direction and Points of Interest for Reflection and Transmission Pressure Readings	12
9 Reflection and Transmission Pressure Waves versus Time at 15 kHz	14

LIST OF ILLUSTRATIONS (Cont'd)

Figure		Page
10	Angles of Incidence	14
11	R and T Coefficients versus Angle of Incidence for a 1-Inch Curved Shell at 15 kHz.....	15
12	R and T Coefficients versus Angle of Incidence for 2-Inch Curved Shell at 15 kHz.....	16
13	SPH Flat Plate Model (at one-fifth the size of the original model to reduce analysis time and size of the results file)	18
14	Closeup of the SPH Model to Show the SPH Particles	18

LIST OF TABLES

Table		Page
1	Material Properties for Linearly-Elastic Materials	6
2	Material Properties for FRP Composite in a Flat Plate Model	7
3	Material Properties for FRP Composite in a Curved Shell Model	7
4	Comparison of Reflection and Transmission Coefficients at 15 kHz and Normal Incidence	19

LIST OF ABBREVIATIONS AND ACRONYMS

2D	Two Dimensional
3D	Three Dimensional
CEL	Coupled Eulerian-Lagrangian
FEA	Finite Element Analysis
FRP	Fiber-Reinforced Polymer
Hz	Hertz
kHz	Kilohertz
ksi	Kilopound per Square Inch
PBM	Physics-Based Modeling
SPH	Smoothed Particle Hydrodynamics

LIST OF SYMBOLS

A	Magnitude of Intermediate Transmitted Acoustic Wave
B	Magnitude of Intermediate Reflected Acoustic Wave
c	Speed of Sound
E	Young's Modulus of Elasticity
G	Shear Modulus of Elasticity
K	Bulk Modulus of Elasticity
k	Wave Number
L	Length of the Middle Fluid Layer (or Thickness of the Plate)
P_i	Magnitude of the Incident Acoustic Wave
P_r	Magnitude of the Reflected Acoustic Wave
p_a	Wave Equation of the Intermediate Transmitted Acoustic Wave
p_b	Wave Equation of the Intermediate Reflected Acoustic Wave
p_i	Wave Equation of the Incident Acoustic Wave
p_r	Wave Equation of the Reflected Acoustic Wave
p_t	Wave Equation of the Total Transmitted Acoustic Wave
R	Reflection Coefficient
$ R $	Magnitude of the Reflection Coefficient
r	Acoustic Impedance
T	Transmission Coefficient
T_I	Intensity Transmission Coefficient
ρ	Density
ν	Poisson's Ratio
ω	Frequency

STRUCTURAL ACOUSTIC PHYSICS-BASED MODELING OF CURVED COMPOSITE SHELLS

1. INTRODUCTION

Understanding sound propagation through curved shell geometries is essential for a wide variety of underwater applications. Specifically, curved shell geometries are found in many naval applications such as acoustic windows, unmanned underwater vehicles, and submarine hulls. This geometry has the potential to reduce acoustic reflections, which makes it an important design feature for Navy products. Often, design requirements for these products focus on reducing the object's susceptibility to undersea detection; so, it is desirable to have the ability to analyze potential designs with regards to this objective.

The development of an acoustic finite element model of a curved shell that can be incorporated into future design analyses would greatly enhance design methods. In addition, ensuring that the model is universal enough to be used for other applications and industries, such as blast/shock mitigation, could greatly enhance the U.S. Navy's capabilities and collaboration opportunities.

Current Navy products that incorporate curved shell geometries are typically made out of linearly-elastic isotropic materials such as steel. However, although steel is very strong, it is also dense (and thus heavy) and does not have great acoustic absorption properties. This makes it very susceptible to undersea detection. Current research in alternative materials is turning towards fiber-reinforced polymer (FRP) composites—composites containing a thermoset or thermoplastic polymer matrix reinforced by carbon, glass, or aramid fibers—for use in applications requiring high strength-to-weight ratios and high load-carrying capabilities. These materials tend to be very strong but very lightweight, and have much better acoustic absorption properties than steel. They can also be customized during the manufacturing process to obtain material properties that meet the needs of specific applications. FRP composites are of particular interest to the Navy because of their potential to reduce weight and undersea detectability while maintaining the high strength of materials like steel.

The finite element method is a powerful tool that can perform a wide variety of analyses. The most common modeling approach is the standard Lagrangian approach, where nodes are specifically defined within a material, and deformation of the material causes a corresponding deformation of the elements. Other alternative modeling techniques are the coupled Eulerian-Lagrangian (CEL) technique and the smoothed particle hydrodynamics (SPH) technique. The CEL approach differs from the traditional Lagrangian approach in that the nodes (not the material) are fixed in space, and the material deforms through a predefined set of elements. The SPH approach is a numerical, meshless technique that represents a material as a set of particles rather than solid elements as in the Lagrangian and CEL techniques. The investigation of these two modeling approaches for use in acoustic analyses is documented in this study.

In addition to investigating the CEL and SPH analysis techniques, this report also documents the comparison of a curved shell geometry to a flat plate geometry, and linearly-elastic isotropic materials (such as steel) to linearly-elastic orthotropic FRP composites. Analytical calculations are performed and compared to all computational results. Comparisons are made and conclusions are drawn concerning the effect of different materials on the absorption and reflection properties of various geometries.

2. PROJECT APPROACH

The overall objective of the study was to use physics-based modeling (PBM) to investigate wave propagations through curved shells that were subjected to acoustic excitation in order to understand the absorption and reflection properties of materials such as FRP composites. To achieve this objective, the first step was to perform analytical calculations to determine the reflection and transmission coefficients for flat plates using both an isotropic, linearly-elastic material (such as steel) and an orthotropic, linearly-elastic composite material.

Flat plate models using the various techniques described earlier (Lagrangian, CEL, and SPH) were then developed and compared to the analytical calculations to determine the validity of these methods for steady-state harmonic excitation analyses that are typical of naval applications. To best assess the capabilities of these methods, the simplest geometries and materials were used in this portion of the project. Specifically, these models were limited to flat plates and a linearly-elastic isotropic material (steel).

Curved plate modeling techniques were then examined using the traditional Lagrangian finite element analysis (FEA) approach. In this stage of the project, both isotropic and orthotropic (composite) materials were examined. In all cases, the FEA results were validated against analytical models to determine the accuracy of the techniques. Transmission and reflection coefficients were then compared between the different plate designs.

3. ANALYTICAL CALCULATIONS

To ensure that the FEA models produce accurate results, it is beneficial to compare them to verified analytical calculations. Kinsler, et al. provide a technique for calculating the reflection and transmission coefficients through a fluid layer at normal incidence.¹ However, calculating these coefficients for curved shells becomes more difficult. Kinsler, et al. provide equations for calculating the reflection and transmission coefficients for plane waves traveling at oblique angles to the interface between two dissimilar fluids, but the model is limited to only two fluids and a single interface. It is possible to extend this model to incorporate a fluid layer; however, the technique fails to address the fact that the incident wave will excite transverse waves in the middle layer (the plate in this case). This becomes a significant issue when considering a curved shell, because as the wave travels through the plate, minute deflections in the plate can cause changes in the incident angle. This in turn will affect the reflection and

transmission coefficients, since the angle of incidence plays a rather large role in oblique calculations. Therefore, performing curved shell analytical calculations was deemed out of the scope of this project and will not be included in this report.

As mentioned above, Kinsler, et al. provides equations for determining reflection and transmission coefficients for a variety of scenarios. This project focuses on the coefficients for a wave traveling through a fluid layer where the middle “fluid” is actually a solid plate (as seen in figure 1 below). At normal incidence, many solids obey the same equations that were developed for fluids. Although the following equations were developed for fluids, they remain valid when considering the middle layer to be a solid.

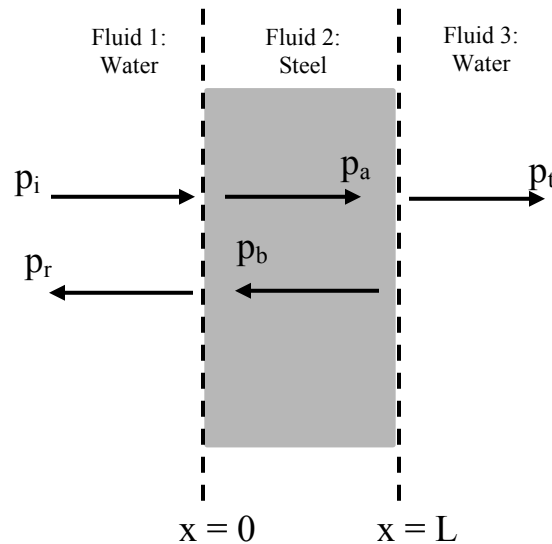


Figure 1. Depiction of Fluid Layer Orientation and Acoustic Wave Transmission

The reflection and transmission coefficients are ratios of the reflected or transmitted pressure waves to the incident pressure wave. Calculating the coefficients begins with a known incident pressure wave (or more specifically the frequency and amplitude thereof). Other requirements for the calculation include the density and speed of sound for both the water and the material of the plate as well as the thickness of the plate:

- ω : frequency (rad/s)
- ρ : density (lb/in³)
- c : speed of sound (in/s)
- L : thickness of plate (in)

These quantities can then be used to determine the characteristic acoustic impedance (r) and wave number (k) of each material:

$$r = \rho * c \quad (1)$$

$$k = \frac{\omega}{c} \quad (2)$$

The wave equations for the incident, reflected, and transmitted waves then become:

$$p_i = P_i e^{i(\omega t - k_1 x)} \quad (3)$$

$$p_r = P_r e^{i(\omega t + k_1 x)} \quad (4)$$

$$p_a = A e^{i(\omega t - k_2 x)} \quad (5)$$

$$p_b = B e^{i(\omega t + k_2 x)} \quad (6)$$

$$p_t = P_t e^{i(\omega t - k_3 x)} \quad (7)$$

where p_i is the incident wave, p_r is the reflected wave, p_a is the wave transmitted into the plate, p_b is the wave reflected off the back face of the plate, and p_t is the wave transmitted into the second fluid domain (see figure 1). All numerical subscripts throughout the calculations refer to the corresponding fluid seen in figure 1. By considering the continuity of the acoustic impedances at $x = 0$ and $x = L$, the amplitudes can then be combined to give:

$$\frac{P_i + P_r}{P_i - P_r} = \frac{r_2}{r_1} \frac{A + B}{A - B} \quad (8)$$

$$\frac{A e^{-ik_2 L} + B e^{ik_2 L}}{A e^{-ik_2 L} - B e^{ik_2 L}} = \frac{r_3}{r_2} \quad (9)$$

Solving the above equations gives the reflection and transmission coefficients:

$$R = \frac{P_r}{P_i} = \frac{\left(1 - \frac{r_1}{r_3}\right) \cos(k_2 L) + i \left(\frac{r_2}{r_3} - \frac{r_1}{r_2}\right) \sin(k_2 L)}{\left(1 + \frac{r_1}{r_3}\right) \cos(k_2 L) + i \left(\frac{r_2}{r_3} + \frac{r_1}{r_2}\right) \sin(k_2 L)} \quad (10)$$

$$T_I = \frac{1}{2 + \left(\frac{r_3}{r_1} + \frac{r_1}{r_3}\right) \cos^2(k_2 L) + \left(\frac{r_2^2}{r_1 r_3} + \frac{r_1 r_3}{r_2^2}\right) \sin^2(k_2 L)} \quad (11)$$

$$\mathbf{T} = \frac{\mathbf{P}_t}{\mathbf{P}_i} = \left(\frac{r_2}{r_1}\right) \left(\frac{r_3}{r_2}\right) \sqrt{T_I} = \left(\frac{r_3}{r_1}\right) \sqrt{T_I} \quad (12)$$

Notice that \mathbf{R} (the reflection coefficient) is actually a complex quantity. In this case, the \mathbf{R} that is used throughout this report is the magnitude of this complex quantity, which is calculated as:

$$|\mathbf{R}| = \frac{\left(\frac{r_2}{r_3} - \frac{r_1}{r_2}\right) \left(\frac{r_2}{r_3} + \frac{r_1}{r_2}\right) \sin^2(k_2 L)}{\left(1 + \frac{r_1}{r_3}\right)^2 \cos^2(k_2 L) + \left(\frac{r_2}{r_3} + \frac{r_1}{r_2}\right)^2 \sin^2(k_2 L)} * \frac{1}{\cos\left(\tan^{-1}\left(\frac{\left(1 + \frac{r_1}{r_3}\right) \cos(k_2 L)}{\left(\frac{r_2}{r_3} + \frac{r_1}{r_2}\right) \sin(k_2 L)}\right)\right)} \quad (13)$$

4. FINITE ELEMENT MODEL DESCRIPTION

4.1 FLAT PLATE MODEL

The model used for all flat plate analyses was a three-dimensional 3-inch by 3-inch rectangular prism that incorporated either a 1-inch or 2-inch plate in the middle (the yellow portion in figures 2 and 3) and 30 inches of water on either side (blue in figures 2 and 3). Overall model dimensions are 3 inches by 3 inches by 61 inches. Along the z-axis, the mesh densities for the plate and water are 0.25 inch and 0.15 inch, respectively. Along the x-axis, the mesh density for both the plate and the water is 0.15 inch. The plate elements are eight-node, linear, brick stress/displacement continuum elements (C3D8R) while the water elements are eight-node, linear, brick acoustic continuum elements (AC3D8). The analyses of the flat plate model were completed using Abaqus/Standard to perform a steady-state dynamic response analysis from 500 Hz to 30,000 Hz.

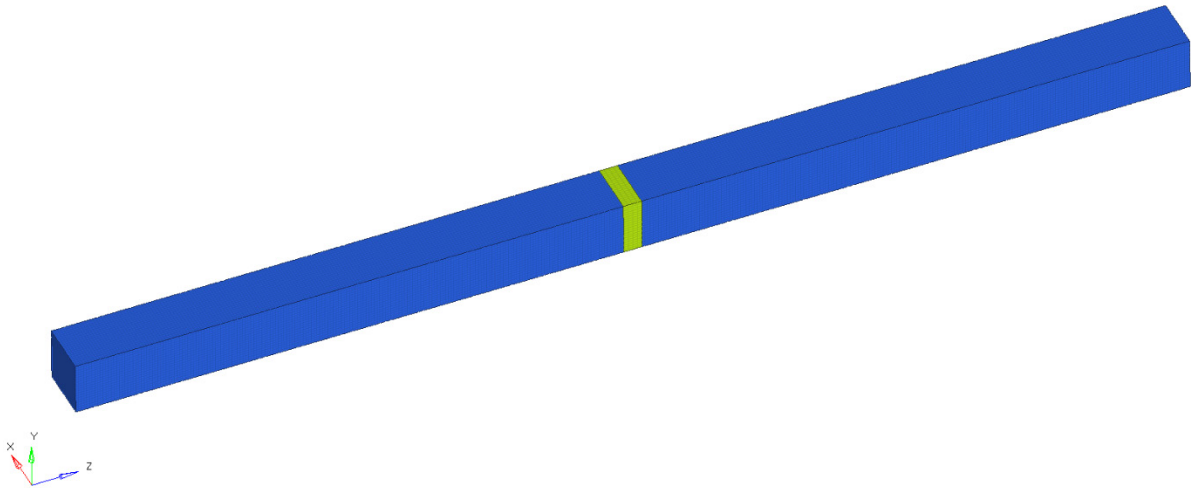


Figure 2. Flat Plate 3D Finite Element Model with a 1-Inch Plate

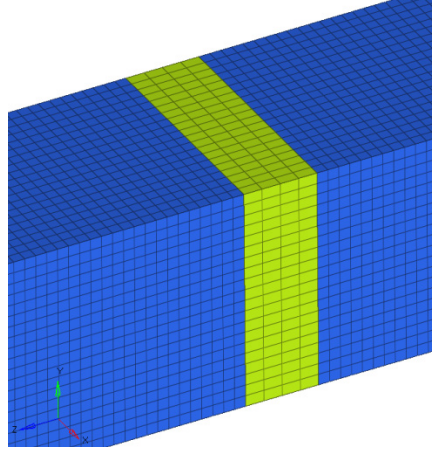


Figure 3. Closeup View of Mesh Refinement for a Flat Plate Model

The faces between the water and the plate are tied (as opposed to equivalenced) to ensure proper transfer of the wave from the water to the plate. Symmetry boundary conditions were imposed on the x - and y -directions on the plate's corresponding surfaces. Impedance boundary conditions were imposed on the $+z$ and $-z$ faces of the water at either end of the waveguide to absorb the acoustic waves exiting the waveguide. The water surfaces normal to the x - and y -axes are assumed to be perfectly reflective (acoustic symmetry boundary conditions). These boundary conditions ensure that the model behaves as if it were an infinite plate submerged in open water. The acoustic wave was formulated as a plane wave that traveled in the positive z -direction. The amplitude of the wave was held constant at 1 npsi throughout all analyses, while the frequency of the wave was varied to see how frequency affected the reflection and transmission of the acoustic wave.

For these analyses, the plate material was either a linearly-elastic isotropic steel or a linearly-elastic orthotropic FRP composite with orientation-dependent properties. FRP composites are stiffer (and stronger) in the direction of the fibers than they are in the through-thickness direction, so it is necessary to define the material properties as such in the analysis. The composite used for these analyses was a generic composite with the fibers aligned in the x - and y -directions, which means the material is strongest in these directions. The material properties for all materials used in the analyses are outlined in tables 1, 2, and 3.

Table 1. Material Properties for Linearly-Elastic Materials

	ρ (lb/in ³)	E (ksi)	K (ksi)	ν	c (in/s)
Steel	7.35822E-04	29007.55	n/a	0.29	198549.60
Water	9.3570E-05	n/a	326.30	n/a	59060

Table 2. Material Properties for FRP Composite in the Flat Plate Model

Composite	
ρ (lb/in³)	1.49595E-04
E1 (ksi)	19000.00
E2 (ksi)	19000.00
E3 (ksi)	1300.00
ν_{12}	0.32
ν_{13}	0.25
ν_{23}	0.25
G12 (ksi)	750.00
G13 (ksi)	750.00
G23 (ksi)	750.00
c (in/s)	93220.87

Table 3. Material Properties for FRP Composite in the Curved Shell Model

Composite	
ρ (lb/in³)	1.49595E-04
E1 (ksi)	19000.00
E2 (ksi)	1300.00
ν_{12}	0.32
G12 (ksi)	750.00
c (in/s)	93220.87

4.2 CURVED SHELL MODEL

The model used for the curved shell analyses was two-dimensional (2D), as opposed to three-dimensional (3D) like the flat plate model. The 2D model shown in figures 4 and 5 represents a slice of a 3D cylinder that extends along the z-axis. Using a 2D model instead of a 3D model is advantageous because it significantly decreases the size of the model and therefore the time it takes to complete the analysis. The approach used here treats the half circle plate as an infinitely long cylinder, and the elements used are plane strain elements that assume there is no strain along the z-axis. This approach is valid for these analyses because, for an infinitely long cylinder, every section along the z-axis will experience the same loading and will produce the same response.

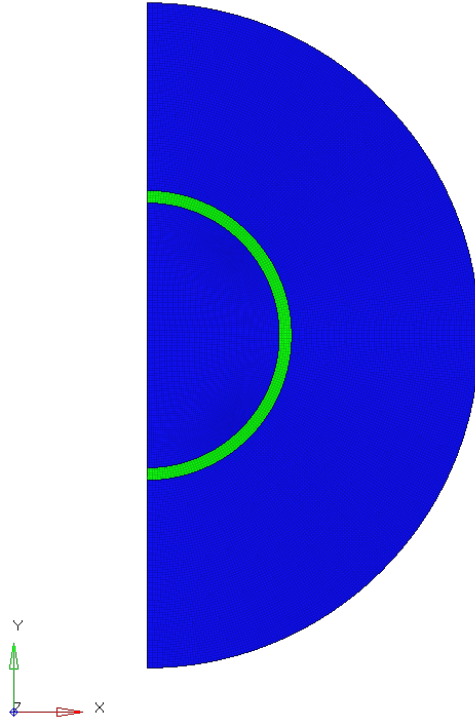


Figure 4. Curved Shell 2D Plane Strain Model with a 1-Inch Shell

The cylinder's inner radius is 10.5 inches and its thickness is 1 inch. The water extends radially from the outside of the plate for 15 inches and the element size for the entire model is approximately 0.2 inch. The plate elements are a combination of plane strain, three-node, linear elements (CPE3) and plane strain, four-node bilinear elements (CPE4R). The water elements are a combination of acoustic, three-node, linear elements (AC2D3) and acoustic, four-node, bilinear elements (AC2D4R).

Similar to the flat plate model, the node-based surfaces between the plate and the water were tied to ensure proper transfer of the wave from the water to the plate. In addition, the incoming plane wave travelled in the negative y-direction. An x-direction symmetry boundary condition was imposed on the model's centerline to act as a rigid wall that caused reflections representing the transmitted wave from the other half of the cylinder. This helped reduce the model size and thus reduce the time and resources required to run the analysis. The impedance boundary condition in this model was applied to the outer surface of the water to ensure that exiting waves did not reflect back towards the plate. In addition, the acoustic wave was defined in the same manner as in the flat plate (except it travels in the negative y-direction), and the materials used were the same as defined previously. However, in this case the composite is 2D with the fibers aligned in the circumferential direction; the one-direction in the material property definition refers to the circumferential direction while the two-direction refers to the through-thickness direction.

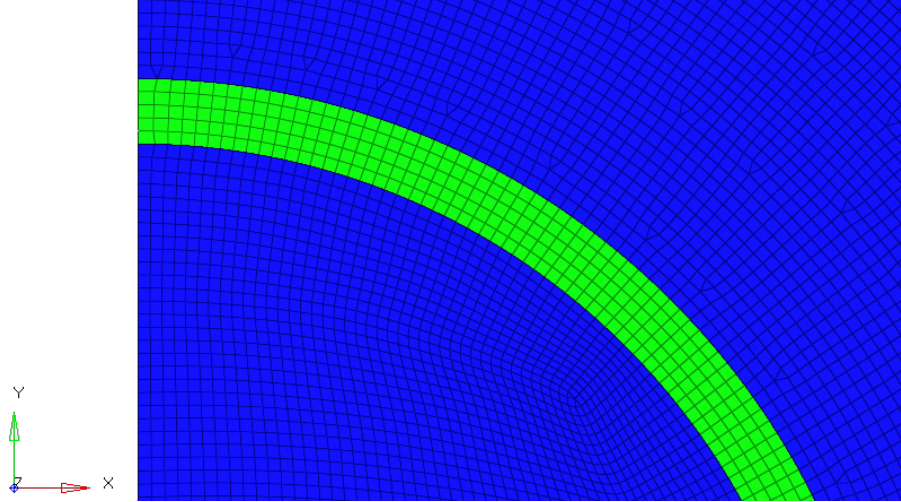


Figure 5. Closeup of a Mesh Refinement in the 1-Inch Curved Shell Model

Despite the curved shell model's similarities to the flat plate model, the setup of the analyses was very different. Whereas the flat plate model analyses were run in the frequency domain, the curved shell model analyses were run in the time domain using Abaqus/Explicit. The total simulation time for the analyses depends on both the distance the wave needs to travel along the waveguide to reach the plate as well as the frequency of the wave. In all explicit analyses, 60 data points per period were used in order to provide the desired level of accuracy in the results (the higher the number of data points, the more accurate the resultant pressure waves).

5. RESULTS

5.1 COMPARISON OF FLAT PLATE COMPUTATIONAL MODELS TO ANALYTICAL CALCULATIONS

Overall, the results from the computational analyses matched the analytical calculations very well; the approximate errors of the computational results when compared to the analytical calculations are all under 1%.

Figure 6 shows that the R and T coefficient curves of the composite plate mirror those of the steel plate; however, the composite material is more acoustically transparent than the steel. In fact, except for the 18 kHz to 29 kHz frequency range, more of the acoustic wave is transmitted through the composite plate than is reflected by it. The steel plate, on the other hand, reflects much more of the incoming wave for frequencies exceeding 2400 Hz.

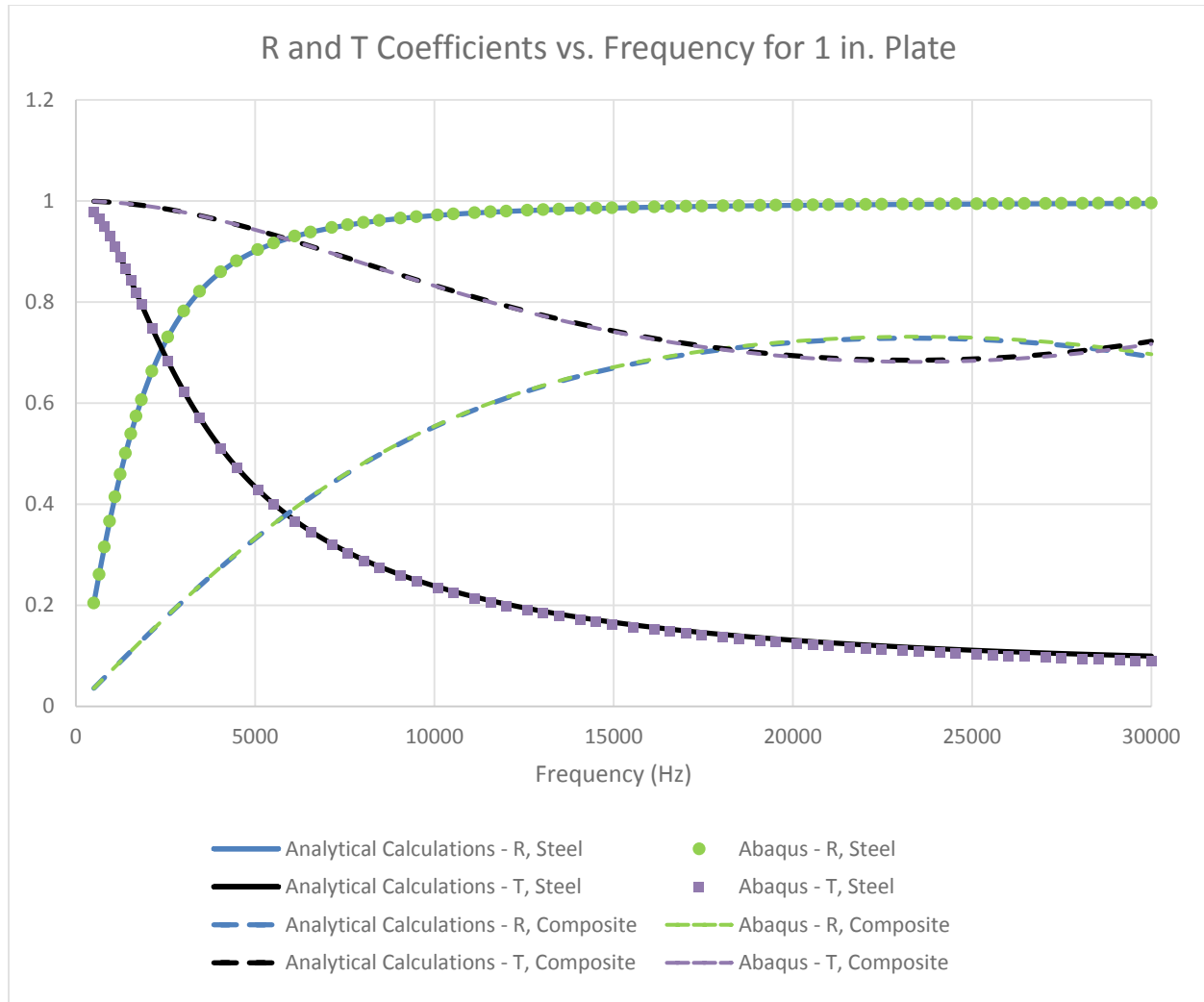


Figure 6. *R* and *T* Coefficients versus Frequency for a 1-Inch Flat Plate

It is interesting to note, however, that these frequency ranges change rather significantly for the 2-inch plate as compared to the 1-inch plate. Figure 7 shows that the range in which more of the acoustic wave is transmitted through the plate (as opposed to reflected from it) for the steel plate is about half of what it was for the 1-inch plate: only 500 Hz to ~1200 Hz. Similarly, for the composite plate, the range is 9 kHz to 14.5 kHz, which again is about half of what it was for the 1-inch plate. This leads to the conclusion that as the thickness of the plate increases, the amount of energy from the incident wave that is transmitted through the plate reduces accordingly. In addition, the graphs in figure 7 clearly show that as the frequency of the wave increases, wave transmission also decreases significantly.

Another interesting phenomenon seen in figure 7 (specifically looking at the composite ***R*** and ***T*** coefficients) is the point at approximately 23 kHz where almost the entirety of the wave is transmitted through the plate. This is most likely related to the wavelength of the wave at that frequency. When the wavelength of the wave is equal to or very close to the thickness of the

plate, the internally reflected wave will cancel out the incoming wave. This results in almost no reflection of the incident wave and, instead, almost perfect transmission.

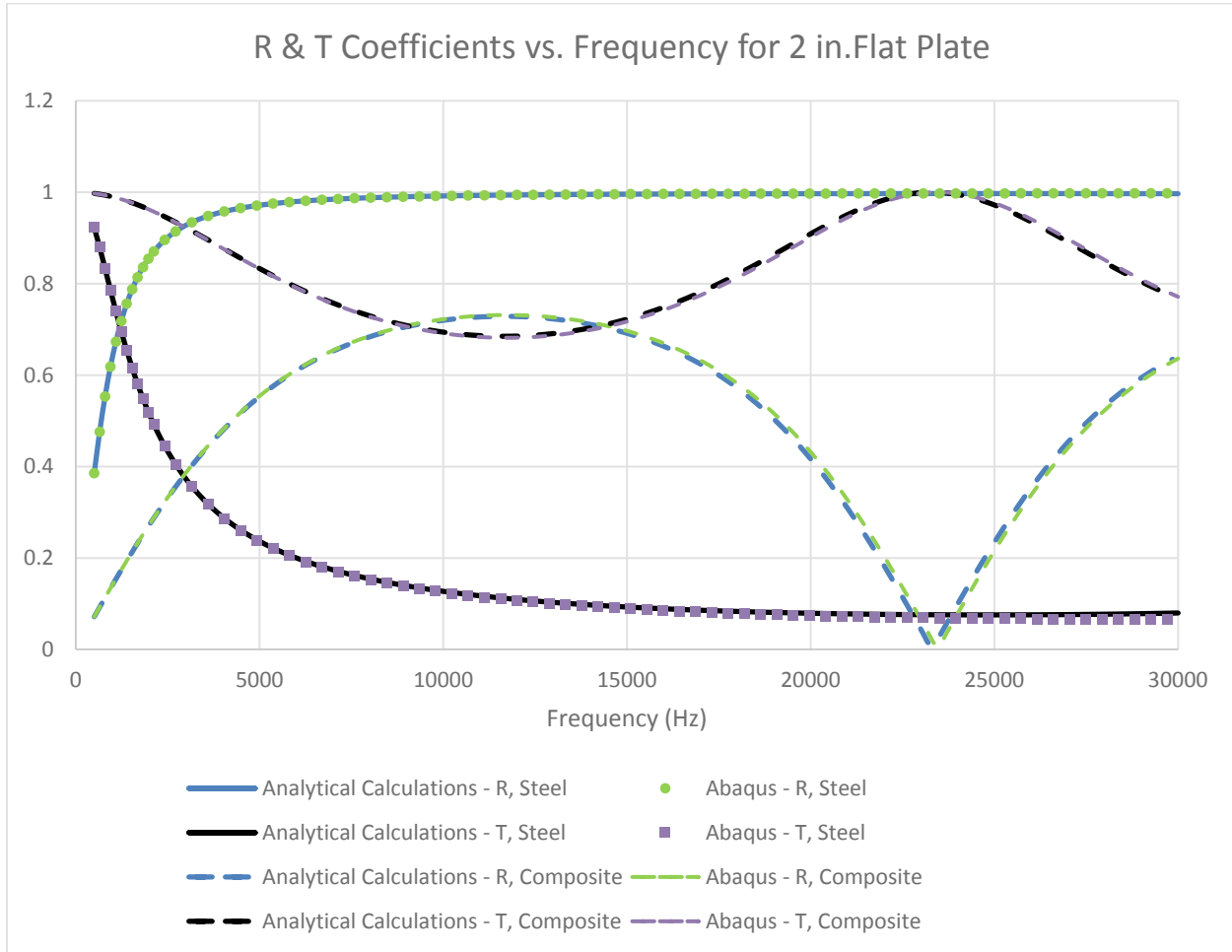


Figure 7. *R* and *T* Coefficients versus Frequency for a 2-Inch Flat Plate

5.2 CURVED SHELL RESULTS

To validate the curved shell model, results along the line at which the angle of incidence is zero (seen on the left side of figure 8) were compared to the flat plate analytical calculations. Explicit analyses were run every 1 kHz from 8 kHz to 30 kHz to ensure that the model was valid and could be trusted throughout a range of frequencies. The results at normal incidence points on either side of the plate (the yellow dots in figure 8) were then compared to the results from the analytical flat plate calculations. These points were chosen because they represent reflection and transmission points along the line at which the incident wave intercepts the plate at zero degrees from the vertical (where the wave comes in exactly normal to the plate).

These results matched very well, with percent errors for the 1-inch steel model within 5% and 8% for *R* and *T*, respectively. The *R* and *T* coefficients for the 1-inch composite curved

shell and the 2-inch steel and composite analyses all matched the flat plate calculations similarly well. This allowed for the conclusion that the model parameters were defined correctly and behaved as expected at normal incidence. The application of analytical expressions to evaluate reflection and transmission coefficients at oblique incidence is beyond the scope of the current tasking. Instead, it was assumed that a fine-scale mesh of the curved surface, used with the Abaqus/Explicit solver, would sufficiently resolve transmission and reflection for off-normal wave incidence.

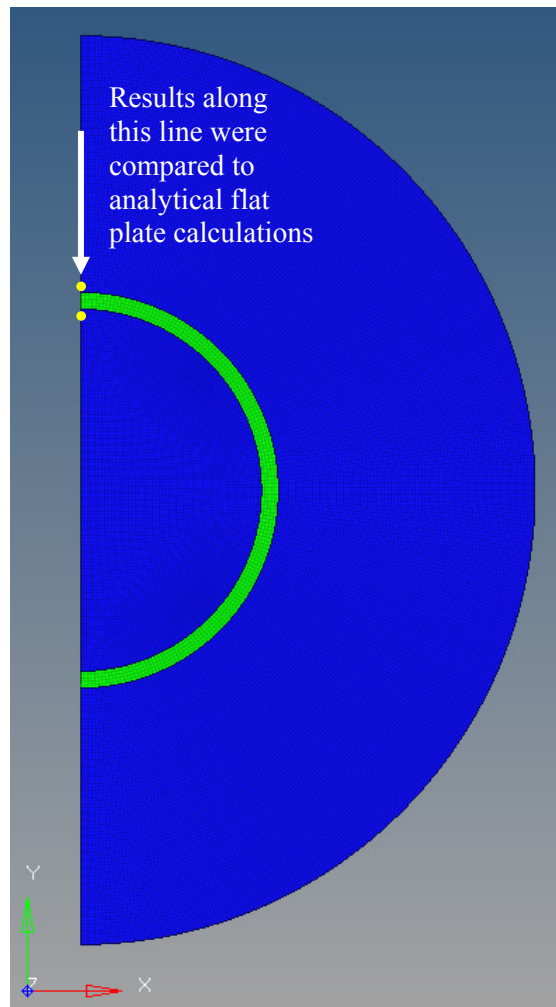


Figure 8. Depiction of Normal Direction and Points of Interest for Reflection and Transmission Pressure Readings

The higher errors for the curved shell analyses compared with the flat plate analyses can be most likely attributed to the different analysis techniques. The flat plate models were run out to steady-state at each frequency to obtain the magnitudes of the reflection and transmission coefficients. This was valid for the flat plate because the plate was modeled as an infinite plate

in an infinite body of water. This means that there were no additional structures or factors that interfered with the motion of the wave.

The curved shell, however, could not be analyzed in the same manner. These analyses had to be run in the time domain due to the nature of the structure. As time progresses, the portion of the wave that gets transmitted through the cylinder wall will get trapped within the cylinder and reflected off the internal surface. This means that the analysis cannot be run out to steady-state because the magnitudes of R and T calculated at steady-state will contain these extra reflections. Therefore, to obtain accurate outputs of the reflection and transmission properties of the cylinder, the results must be limited to the time occurring prior to when the wave reflects back towards the top of the cylinder.

The results of the explicit analysis come in the form of sine waves for each of the points of interest (i.e. a sine wave for the reflected wave and a sine wave for the transmitted wave). The points at which results were obtained are shown as yellow in figure 8. For example, figure 9 shows the results at these points from the 15 kHz analysis of a 1-inch-thick cylinder. The area of interest in this graph is between 0.0005 seconds and approximately 0.0013 seconds. This portion of the graph represents the segment of time before the wave reflects back from the bottom of the cylinder. It is the amplitude of the wave throughout this section that represents the actual reflection and transmission properties of the cylinder. In order to extract these parameters, the average amplitude of that section of the wave was calculated by averaging the peaks in that section. However, this technique of finding the amplitude of the curve by averaging its peaks can also be a potential source of error in the calculations of R and T and can potentially explain the difference in values between the curved shell analyses and the flat plate calculations.

Another potential source of error when comparing the curved shell computational models to the flat plate analyses is the elastic waves that get excited when the plane wave hits the curved surface. The flat plate model represents an infinite plate in which only dilatational waves are excited. There are no elastic waves travelling within the plate except in the through-thickness direction (i.e. at normal incidence). However, when the plane wave interacts with the curved shell model, elastic waves are excited in addition to the dilatational waves. The analytical solutions do not take these additional elastic waves into account when considering the vibrations of the plate, where in reality they can cause additional radiated pressures from the plate. Since the curved shell pressures will include not only the reflections or transmissions from the shell but also the pressure caused by vibrations due to the internal wave interferences, the curved shell results will be slightly different than both the flat plate computational models and the flat plate analytical models.

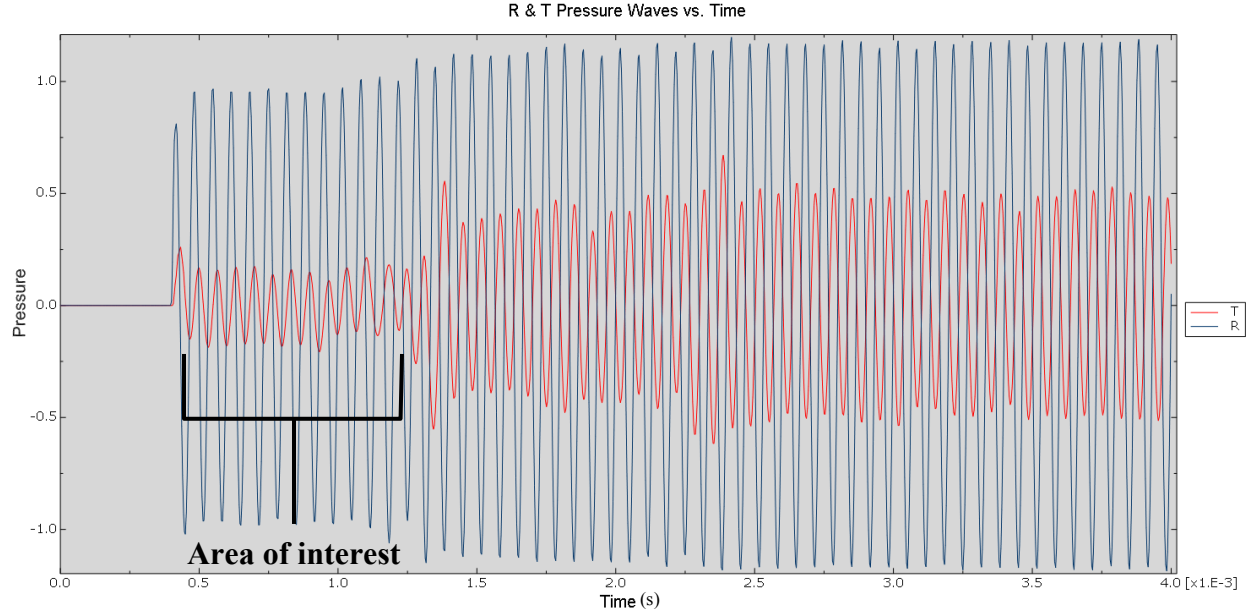


Figure 9. Reflection and Transmission Pressure Waves versus Time at 15 kHz

After concluding that the curved shell model was valid based on the comparison to the flat plate calculations, results from various points around the curve were then analyzed to see how the angle of incidence affected the reflection and transmission coefficients. As the incident wave travels in the negative-y direction it intersects different points on the cylinder at different angles of incidence due to the curvature of the shell. Although this wave excites the structure internally, the resulting response does not have a significant impact on the reflection and transmission coefficients. The angles used in figures 11 and 12 represent the location of the point of interest as compared to the point at normal incidence. This means that the angles are measured from the vertical, as shown in figure 10.

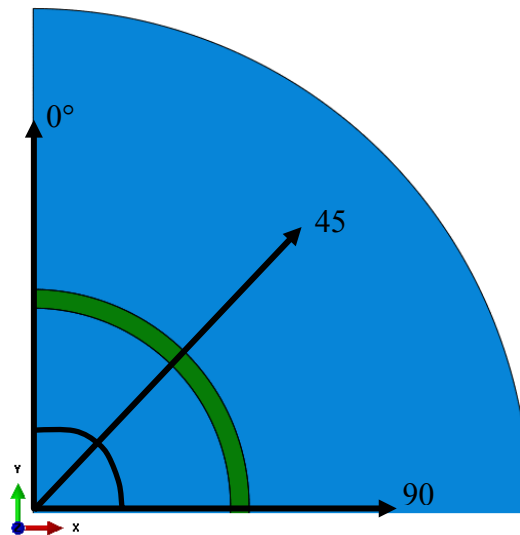


Figure 10. Angles of Incidence

The following graphs (figures 11 and 12) show how the R and T coefficients change as the angle of incidence changes. The coefficient data was extracted from nodes along a path around the cylinder at the frequency of interest (15 kHz). All four of the analyses showed that as the angle of incidence increases, R decreases while T increases. The steel curves and composite curves in both graphs follow similar paths albeit being offset by about 0.2 for the R curves and about 0.6 for the T curves. It is easy to see that the change in material creates a drastic change in the reflection and transmission properties of the geometry. In figure 11, the change in material not only creates more variation in the coefficients as the angle of incidence increases, but it also decreases the angle at which the reflection coefficient begins increasing again. This interesting phenomenon can be seen in all curves except for the 1-inch transmission coefficients; however, further investigation would be required to fully understand why it occurs. It is also worth noting that this occurs much earlier along the curve in the 2-inch shells than it does in the 1-inch shells, which implies that it may also depend on the thickness of the shell itself.

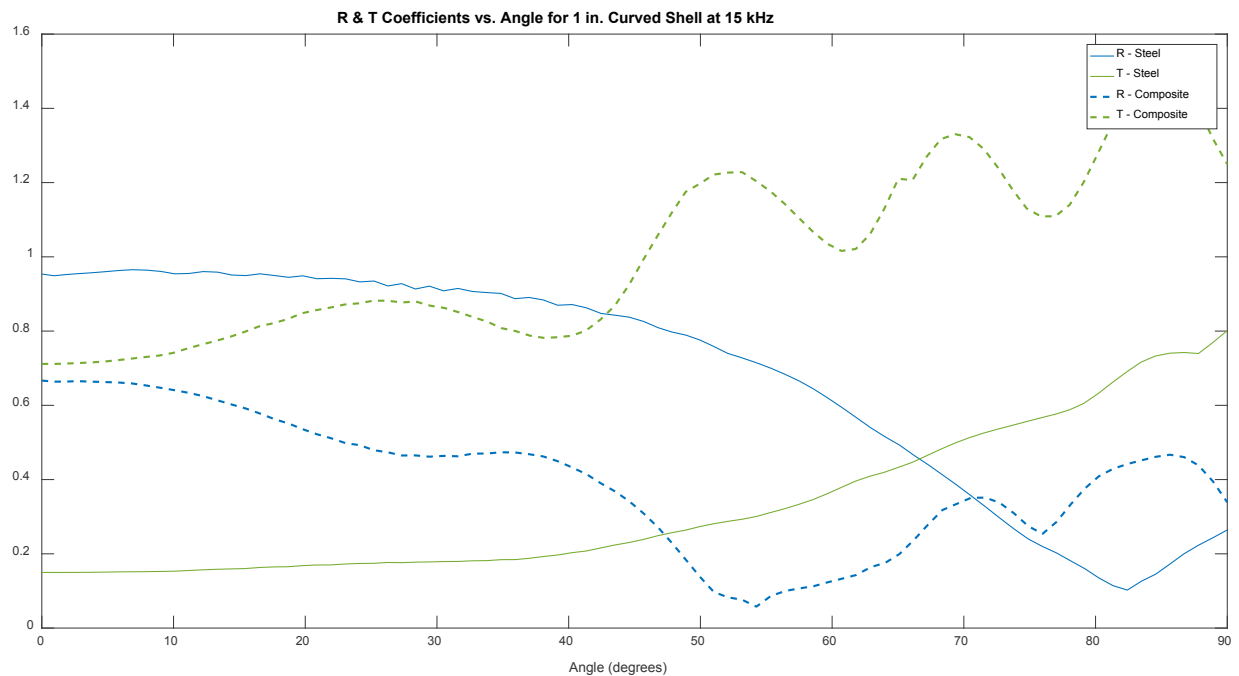


Figure 11. R and T Coefficients versus Angle of Incidence for a 1-Inch Curved Shell at 15 kHz

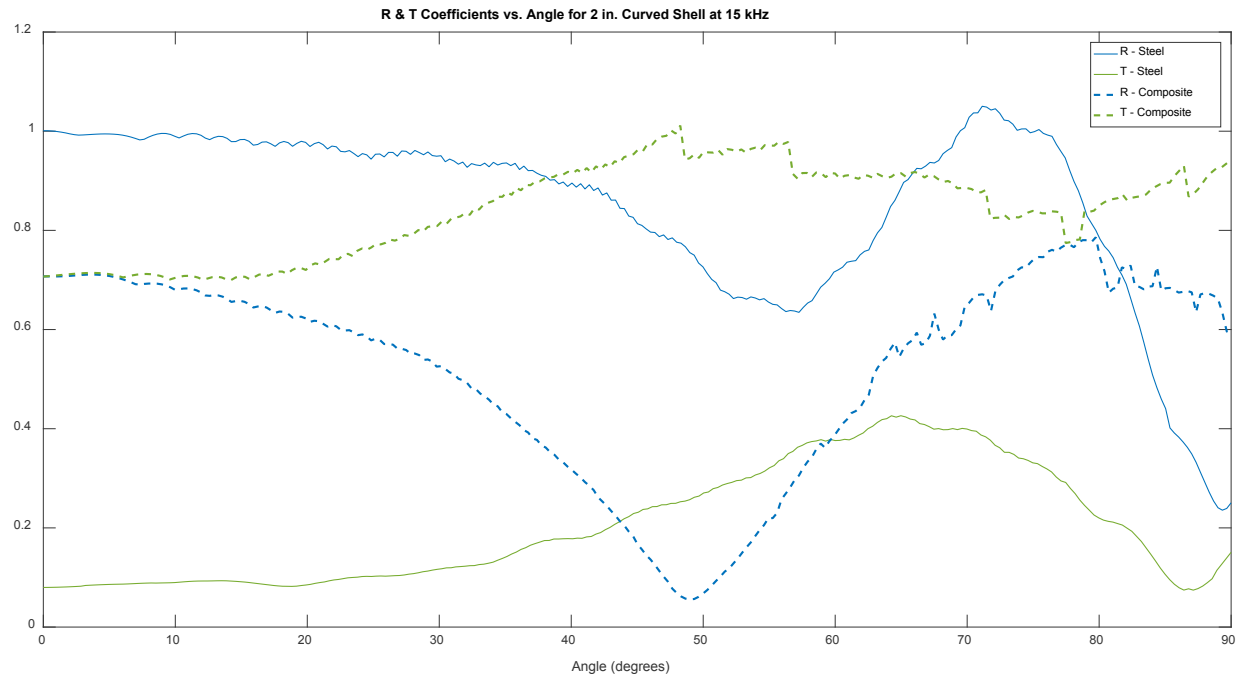


Figure 12. *R and T Coefficients versus Angle of Incidence for 2-Inch Curved Shell at 15 kHz*

6. CEL/SPH ANALYSIS TECHNIQUES

6.1 COUPLED EULERIAN-LAGRANGIAN ANALYSIS

The first additional analysis technique investigated in this project was the coupled Eulerian-Lagrangian (CEL) technique. Traditionally, the elements used in finite element analyses are entirely Lagrangian. The elements are assigned one specific material and as that material deforms throughout the analysis, so do the elements. The elements are always 100% filled with that material, so the boundary of the material is the same as the boundary of the element. Eulerian elements, on the other hand, behave much differently. It is not the elements themselves that deform, but rather the material that deforms and flows through the elements. In addition, elements are not always 100% full of material; they could be only partially filled or entirely void. This means that the boundary of the material must be recomputed at each step in the analysis as it typically does not correspond to the boundary of an element. Eulerian meshes are thus typically defined as a rectangular grid that extends far beyond the boundary of the material. This allows the material to expand and deform throughout the grid as the analysis progresses. However, any material that moves outside of the predefined mesh is lost from the simulation, so the size of the Eulerian mesh must be carefully calculated to ensure that the expansion of the material is properly captured and maintained throughout the analysis.²

The basis of CEL analyses is the interaction of these Eulerian elements with the traditional Lagrangian elements. This technique is commonly used for fluid-structure interactions and analyses that involve very large scale deformations of a structure or material. This analysis technique is better suited for these types of analyses because the Lagrangian elements will become distorted and less accurate. Therefore, since the Eulerian elements are designed to handle these types of deformation and material flow, an analysis technique that allows for the interaction between the two element types is preferred.²

After further investigation and many failed analysis attempts, it was concluded that the CEL analysis approach is not valid for this type of acoustic analysis when using the Abaqus software package. There were a variety of complications that could not be easily resolved, some of which were based on how acoustic waves are defined and transmitted from one element set to another. For example, although contact definition between the Lagrangian and Eulerian elements is possible and typically required for CEL analyses, in this particular case further intensive investigation would be necessary to determine the appropriate contact definition between the two element types. In fact, the type of contact required for transfer of the wave from the water to the plate may not even be possible between Lagrangian and Eulerian elements within Abaqus.

6.2 SMOOTHED PARTICLE HYDRODYNAMICS ANALYSIS

The smoothed particle hydrodynamics (SPH) analysis technique is a meshless numerical method that uses a collection of points (called particles or pseudo-particles) to represent a body, rather than elements. These particles can either be defined when creating the model or converted from traditional finite elements to particle elements during the analysis. This type of mesh is beneficial for fluid flow problems and structural problems that involve large deformations or free surfaces. SPH analyses are, for the most part, set up in a similar fashion to Lagrangian analyses. The same materials, initial conditions, boundary conditions, and contact interactions are used in SPH analyses as in Lagrangian analyses. However, it is important to note that this technique is often less accurate than typical Lagrangian analyses when the deformation is small. Additionally, even when the deformation is large, it can be less accurate than the CEL approach. SPH is best suited for extreme deformation situations such as fluid sloshing, spraying, gas flow, and obliteration/fragmentation that includes secondary impacts.²

One important constraint of SPH particles is that, since they don't have faces or edges like traditional Lagrangian elements do, they cannot be used to define an element-based surface. This means that constraints created using element-based surfaces cannot be defined for SPH particles. However, they can be used to create node-based surfaces, so that interactions such as ties or contact are still possible. Another constraint that was important in regards to this project in particular was the limited output variables associated with these particles. Although most of the typical outputs can be requested using SPH particles, since they are not acoustic elements, they have no pressure degree of freedom and therefore no pressure output.² That aspect presented a problem for the analyses discussed throughout this project because all data obtained and analyzed were pressure data. However, one potential solution for this problem is to obtain

the velocity of the particle of interest and use the velocity data to calculate pressure, which would then in turn provide the R and T coefficients.

The SPH model created for the acoustic analysis (seen in figures 13 and 14) replaced the Lagrangian elements representing the water with SPH particles with 0.15-inch spacing to match the plate's mesh density. Since SPH particles are not acoustic elements, the analysis could not be defined in the same manner as the previously discussed analyses. Instead, an initial velocity was applied to the top face (figure 13) with the same amplitude that was used in the previous analyses. Unfortunately, although the analysis ran successfully, the velocity results on either side of the plate did not match theoretical predictions. Modifications were made to the model to attempt to correct the issue; none of the proposed fixes solved the problem. It was then determined that trying to solve the issue, if even possible, was not within the scope of the project and the SPH analysis technique was deemed not viable for this type of acoustic analysis.

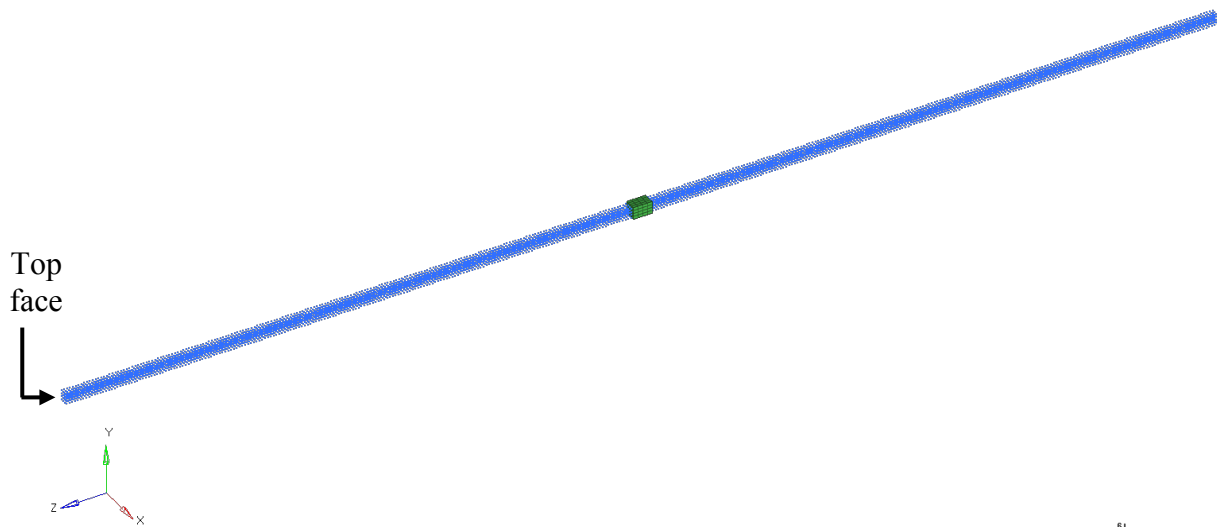


Figure 13. SPH Flat Plate Model (at one-fifth the size of the original model to reduce analysis time and size of the results file)

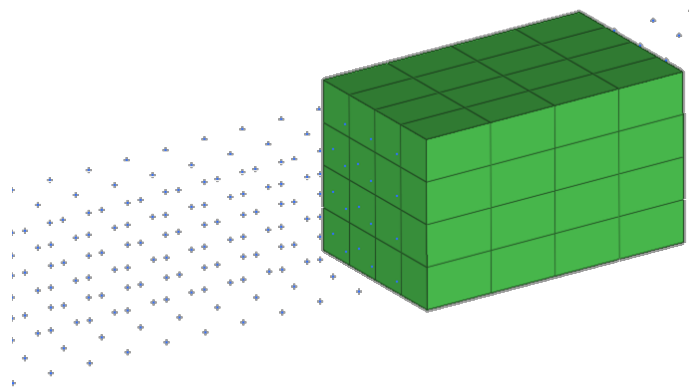


Figure 14. Closeup of the SPH Model to Show the SPH Particles

7. CONCLUSION

For this project, analytical calculations were completed for an acoustic plane wave hitting a flat plate at normal incidence. Finite-element models were created for both flat plate geometry and curved shell geometry, and acoustic analyses were completed. The flat plate model was created using 3D elements and was analyzed in the frequency domain, while the curved shell model was created using 2D elements and was analyzed in the time domain. Two instances of each model were created: one with a 1-inch-thick plate and one with a 2-inch-thick plate. Each of these instances was then analyzed first with a steel plate and then with a composite plate. All analysis results were compared with the analytical calculations to determine accuracy and validity of the model. The flat plate computational models matched the analytical calculations within approximately 1%, while the curved shell computational models matched the analytical calculations within approximately 8%. Table 4 sums up a comparison of the R and T coefficients at 15 kHz and normal incidence for each type of analysis that was run.

Table 4. Comparison of Reflection and Transmission Coefficients at 15 kHz and Normal Incidence

	Steel		Composite	
	R	T	R	T
1-in. flat plate	0.986656	0.162049	0.669250	0.748722
2-in. flat plate	0.995875	0.089352	0.696696	0.717144
1-in. curved shell	0.957258	0.167168	0.666668	0.711760
2-in. curved shell	0.992257	0.080587	0.708405	0.705696

This report also investigated the validity of using CEL and SPH modeling approaches for the discussed acoustic analysis. Unfortunately, issues arose during the application of these approaches, so they were both determined to be unviable techniques at this time for this type of analysis.

This research demonstrated the ability to create and analyze an acoustic model of a curved shell that accurately matches analytical calculations of reflection and transmission coefficients at normal incidence. In addition, comparing the R and T coefficients between steel and the FRP composite provides a better understanding of the absorption and reflection properties of the composite material. In the future, this knowledge can help enhance design methods for future Navy products. In addition, the model developed in this study can be used with confidence in future acoustic analyses to understand an object's susceptibility to undersea detection. This can help drive future research on using composite materials for a wider variety of Navy applications.

REFERENCES

1. Kinsler, Lawrence E., et al. *Fundamentals of Acoustics*. 4th ed., John Wiley & Sons, New York, NY, 2000.
2. *Abaqus 6.14 Documentation*, Dassault Systèmes, Waltham, MA, 2014.

INITIAL DISTRIBUTION LIST

Addressee	No. of Copies
Center for Naval Analyses	1
Defense Technical Information Center (DTIC)	1
U.S. Army Natick Soldier Research, Development, and Engineering Center, Natick MA (M. Jee, G. Proulx)	2